

## Synthesis and Properties of Ionically Modified Polymers with LCST Behavior

Mathias Hahn,<sup>\*,†</sup> Eckhard Görnitz,<sup>†</sup> and Herbert Dautzenberg<sup>‡</sup>

Fraunhofer Institute for Applied Polymer Research, Kantstrasse 55, D-14513 Teltow, Germany, and  
Max-Planck Institute for Colloid and Interface Science, Kantstrasse 55, D-14513 Teltow, Germany

Received January 2, 1998; Revised Manuscript Received June 12, 1998

**ABSTRACT:** Ionically modified LCST polymers were synthesized by free radical copolymerization of *N*-isopropylacrylamide (NIPAM) with various cationic, anionic, and amphoteric comonomers, resulting in products with comparable molecular masses and charge concentrations. The temperature-dependent phase transition behavior of the copolymers was investigated in water, aqueous sodium chloride solutions, and mixtures of water with dimethylformamide (DMF) using light transmission measurements, static light scattering, viscometry, and sedimentation experiments in an analytical ultracentrifuge. The LCST of the cationic modified copolymers remains unchanged compared with the homopolymer, but it is increased as a result of an amphoteric or anionic modification. Phase transitions are accompanied by conformational changes followed by aggregation processes. These changes are enhanced in the presence of salt. The phase transition of poly-NIPAM-*co*-MADAMBQ ((methacryloyloxy)ethyl)dimethylbenzylammonium chloride) in 0.5 M NaCl was studied in detail investigating the temperature dependence of molecular parameters as intrinsic viscosity, particle mass, radius of gyration, second virial coefficient, and sedimentation coefficient.

### Introduction

Materials responding external stimuli have become of major interest in the past decade. Above all, thermoresponsive polymers were objectives of comprehensive investigations both in approaches of theoretical explanations of the phase transition behavior and also in developing novel application fields for this class of polymers.

Thereof, poly(*N*-isopropylacrylamide) (PNIPAM), which is water soluble at low temperatures but shows phase separation when the temperature is raised above the LCST (lower critical solution temperature) of about 32 °C, is the most studied polymer.<sup>1–8</sup> The phase transition temperature of PNIPAM can be changed by cosolvents. In aqueous solutions the presence of an electrolyte leads to an increase of the cloud point,<sup>9</sup> and otherwise, the addition of an organic solvent to the aqueous phase results in a decrease of the LCST.<sup>10</sup>

In the same manner, the incorporation of hydrophilic (nonionic or ionic) units or hydrophobic ones in the NIPAM-polymer structure causes comparable effects, an increase or decrease of the cloud point temperature.<sup>11–14</sup>

The objectives of this work were the synthesis of a series of ionically modified NIPAM copolymers with various cationic, anionic, and amphoteric functional groups and the study of these copolymers in water, in aqueous salt solutions, and in solvent mixtures of water and dimethylformamide. Besides a screening check of the temperature behavior of all synthesized copolymers, the properties of one of the cationically modified NIPAM copolymers were investigated in detail.

### Experimental Section

**(a) Materials.** The monomers NIPAM (Aldrich), sodium acrylate (Aldrich), sodium methacrylate (Aldrich), and sodium

2-acrylamido-2-methylpropanesulfonate (AMPS, Aldrich) (all reagent grade) were used without further purification. Methacryloyloxyethyl–dimethylbenzylammonium chloride (MADAMBQ) (75% aqueous solution) and ((methacryloyloxy)ethyl)–trimethylammonium chloride (MADAMMQ) (75% aqueous solution) were purchased from Nalco Chemical Corp. as technical grade reagents. ((Methacryloyloxy)ethyl)dimethyl ammonium propiobetaine was synthesized by quaternization of 2-(dimethylamino)ethyl methacrylate (Aldrich) with propiolactone in dry acetone. The amine derivative was mixed with the solvent (1:3) in a three-necked flask with stirrer, gas inlet tube, and reflux condenser, and the equimolar amount of propiolactone was added at room temperature under nitrogen at constant reaction temperature. Stirring was continued overnight before the crystallized salt was separated by filtration. The product was dried over phosphorus pentoxide in an exsiccator. The monomer was characterized by <sup>13</sup>C-NMR spectroscopy.

Ammonium persulfate (Merck) was recrystallized in water prior to use. *N,N,N,N*-tetrakis(2-hydroxypropyl)propylenediamine was synthesized by alkylation of propylenediamine with propylene oxide according to the general procedure of Lundstedt.<sup>15</sup>

**(b) Copolymer Synthesis.** All polymerizations were carried out in a 250 mL double jacket glass reactor fitted with a nitrogen bubbling tube, stirrer, reflux condenser, and thermometer. The monomer mixtures were always prepared as 1 M solutions in water, and the fraction of ionic monomer in the monomer mixture was in each case 9 mol %.

To 150 mL of the monomer solutions was added  $2 \times 10^{-3}$  mol/L of the amine activator, and the mixtures were filled into the reactor and thermostated on 25 °C under stirring at 150 rpm. After purging with nitrogen for 30 min,  $1 \times 10^{-3}$  mol/L ammonium persulfate as a 10% solution in water was dosed, and the polymerizations were continued for 2 h at this temperature. The copolymer solutions were diluted to 10 L with water, and the residual monomer and initiator were removed by ultrafiltration (Centrasette, Pall-Filtron) using a membrane cassette of 10000 Da. The purified copolymers were isolated by freeze-drying (Gamma 2-20, Christ). Copolymer compositions were obtained by potentiometric titrations and by <sup>13</sup>C-NMR spectroscopy.

\* To whom correspondence should be addressed.

<sup>†</sup> Fraunhofer Institute for Applied Polymer Research.

<sup>‡</sup> Max-Planck Institute for Colloid and Interface Science.

**(c) Characterization of Copolymer Solutions and Colloidal Properties.** The phase transition behavior was investigated by measurement of the temperature dependence of the optical transparency of the polymer solutions. Therefore, a spectrophotometer (Specol 11, Zeiss Jena) was equipped with a temperature controlled optical cell (optical path length 12.8 mm), and the light transmission at  $\lambda = 546$  nm of the magnetically stirred solutions was recorded together with the directly measured solution temperature. After adjustment of the light transmission at 20 °C to 100% for the corresponding solution, a temperature program with repeating heating and cooling cycles (rates 7 K/min) was started. From the resulting plots the cloud point temperatures for heating and cooling can be derived and the optical transparency (%) of the solution at a stationary state well above the LCST can be determined.

Solution viscosity was recorded using Ubbelohde-type capillary viscometers with automatic dilution (Lauda Viscoboy and Sematech TI1) and evaluated by a Huggins plots according to

$$\frac{\eta_{\text{spec}}}{c} = [\eta] + k_H[\eta]^2 c \quad (1)$$

Static light scattering (SLS) experiments were carried out with a Sofica 42000 instrument (Wippler and Scheibling, Strasbourg, France), which was equipped with a 5 mW He-Ne laser as light source and a PC for data recording. The accuracy of the measurements was better than 1%.

For the screening measurements regarding the cloud point of the various samples in pure water the solutions were made roughly dustfree by filtration through 5  $\mu\text{m}$  membrane filters, leaving traces of particulate material in the solutions. To characterize the macromolecular parameters of the sample AIFL2 in 0.5 M NaCl, the influence of filtration through filters of different pore size was checked, revealing the necessity of severe filtration conditions. To obtain a Zimm diagram a stock solution was filtered in succession through 5, 1.2, and 0.45  $\mu\text{m}$  filters to avoid a blocking of the membranes, and the set of diluted solutions were once more filtered through 1.2  $\mu\text{m}$  filters to make them dustfree.

For data analysis the refractive index increment of polyacrylamide ( $dn/dc = 0.189$  mL/g) was used for the measurements in pure water, which should be justified because of the low content of the comonomers. For the sample AIFL2 in 0.5 M NaCl the value  $dn/dc = 0.169$  mL/g was determined after dialysis with the interferometric refractometer ScanRef (Nanofilm Technologie GmbH, Göttingen, Germany).

The partial specific volume  $\bar{v}$  was determined from the concentration dependence of the solution density with the densimeter DMA 60/602 (Anton Paar, Graz, Austria).

Analytical ultracentrifugation (Optima XL-I, Beckman Instruments, Palo Alto, CA) was used for the determination of the sedimentation coefficients of the polymeric species by means of sedimentation velocity experiments as well as for the determination of the absolute molecular mass in sedimentation equilibrium experiments.

Velocity runs were carried out at different temperatures with 1.84 mg/mL polymer in 0.5 M NaCl buffer at 45000 rpm for  $T \leq \text{LCST}$  and at 5000 rpm for  $T > \text{LCST}$  and evaluated with respect to the mean apparent sedimentation coefficients  $S_{\text{app}}$  and the sedimentation coefficient distributions  $g(s)$  according to Stafford.<sup>16</sup>

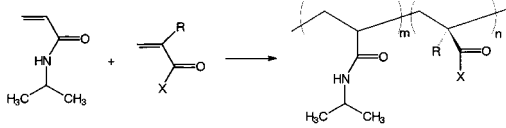
Sedimentation equilibrium was investigated with 6 concentrations in the range 0.2–1.3 mg/mL (dialyzed solutions in 0.5 M NaCl) in two 6-cannel Yphantis-style cells with 12 mm optical path length (filling height 2 mm) at 5000 rpm subsequently at different temperatures in one run over 120 h. The equilibrium concentration profiles were scanned by means of the interference optical system of the Optima XL-I and evaluated with respect to weight- and z-averaged molecular mass and second virial coefficient as described elsewhere.<sup>17</sup>

## Results and Discussion

### (a) Copolymer Synthesis and Characterization.

Scheme 1 represents the series of ionically modified

**Scheme 1. Structure and Specification of the Synthesized Copolymers**



Sample	-R	-X
AIFL1	-CH <sub>3</sub>	-OCH <sub>2</sub> CH <sub>2</sub> N <sup>+</sup> (CH <sub>3</sub> ) <sub>3</sub>
AIFL2	-CH <sub>3</sub>	-OCH <sub>2</sub> CH <sub>2</sub> N <sup>+</sup> (CH <sub>3</sub> ) <sub>2</sub> Cl <sup>-</sup> CH <sub>2</sub> C <sub>6</sub> H <sub>5</sub>
AIFL3	-H	-NHC(CH <sub>3</sub> ) <sub>2</sub> CH <sub>2</sub> SO <sub>3</sub> <sup>-</sup> Na <sup>+</sup>
AIFL4	-H	-O <sup>-</sup> Na <sup>+</sup>
AIFL5	-CH <sub>3</sub>	-O <sup>-</sup> Na <sup>+</sup>
AIFL6	-CH <sub>3</sub>	-NH(CH <sub>2</sub> ) <sub>3</sub> N <sup>+</sup> (CH <sub>3</sub> ) <sub>2</sub> CH <sub>2</sub> CH <sub>2</sub> COO <sup>-</sup>
AIFL7		Homopolymer NIPAM

**Table 1. Polymerization Results, Copolymer Composition, and Viscosimetric Data (30 °C, 1 M NaCl)**

sample	polymerization conversion (%)	mol % of ionic component	$[\eta]$ (mL/g)	$k_H$
AIFL1	22.4	7.33	245.3	0.58
AIFL2	24.1	7.54	221.6 <sup>a</sup>	0.53 <sup>a</sup>
AIFL3	19.1	6.02	259.8	0.45
AIFL4	18.4	5.89	269.7	0.41
AIFL5	18.7	5.85	213.6	0.45
AIFL6	20.8	6.75	179.0	0.41
AIFL7	27.5	0	236.0 <sup>a</sup>	0.57 <sup>a</sup>

<sup>a</sup>  $T = 22.5$  °C; solvent 0.5 M NaCl.

NIPAM copolymers synthesized for the further investigations. The conditions of the copolymer preparation and the molecular properties of the various ionic groups containing LCST polymers are given in Table 1. Similar polymerization conversions and, corresponding to it, comparable mole fractions of ionic groups in the copolymers of about 6–7 mol % show that the reactivity ratios of the various comonomer pairs are nearly the same. Furthermore, the intrinsic viscosities calculated from the Huggins plots lie also in the same order of magnitude and the corresponding Huggins coefficients  $k_H$  show the expected values around 0.55 for the NIPAM homopolymer and the cationically modified polymer products and 0.4–0.45 for the various anionic derivatives and the amphoteric copolymer.

Due to phase separation at the applied standard conditions (30 °C, 1 M NaCl) in the case of the copolymer AIFL2 and the NIPAM homopolymer (AIFL7) the viscosity measurements were performed in 0.5 M sodium chloride solution and at lower temperature.

**(b) Aggregation Behavior of the Copolymer Solutions. (i) Studies in Pure Water.** At first the temperature-dependent phase separation behavior of the various copolymer systems was investigated in pure water. In the aqueous solutions of the cationically modified poly-NIPAM's phase separation could be induced by continuous increase of the temperature up to the corresponding cloud point temperature. The same properties were found for the amphoteric copolymer and the NIPAM homopolymer.

Figure 1 represents an example of such phase separation behavior over several heating and cooling periods

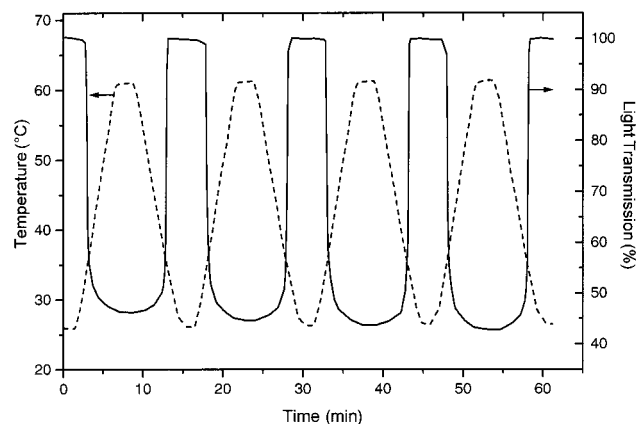


**Figure 1.** Switching behavior of the copolymer sample AIFL2 (5 g/L in deionized water) over several heating and cooling periods.

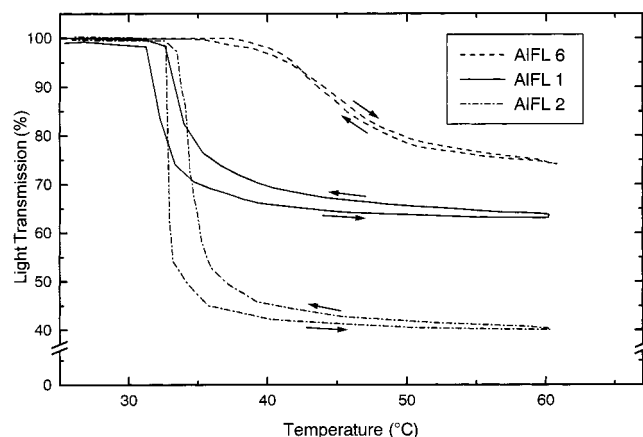


**Figure 2.** Phase behavior of 5 g/L aqueous solutions of the ionically modified NIPAM copolymers AIFL1, AIFL2 (both cationic), and AIFL6 (amphoteric) during a heating/cooling cycle, light transmission vs temperature plot.

**Table 2. Phase Transition Temperatures of the Ionically Modified NIPAM Copolymers in Diluted Aqueous System (5 g/L in Water)**

sample	phase transition temp (°C)	light transmn at 60 °C (%)
AIFL1	32.5	65
AIFL2	33.0	40
AIFL3	>90	100
AIFL4	>90	100
AIFL5	>90	100
AIFL6	43.0	75
AIFL7	32.3	nd <sup>a</sup>

<sup>a</sup> Not detectable due to the fast association of the primary particles.

in the temperature range between 25 and 60 °C for an aqueous solution of the copolymer AIFL2. The switching behavior remains constant over a large number of cycles and is nearly identical during heating and cooling, as it is demonstrated by the light transmission versus temperature plots in Figure 2. Table 2 contains the phase transition temperatures of the various polymer samples estimated from the heating phase, as well as the light transmission measured at 60 °C. Although, more than 6 mol % of cationically charged comonomer is incorporated into the macromolecular chains, no shifting of the cloud point temperature was observed in comparison to the NIPAM homopolymer. On the other hand, in the case of the amphoteric copolymer the

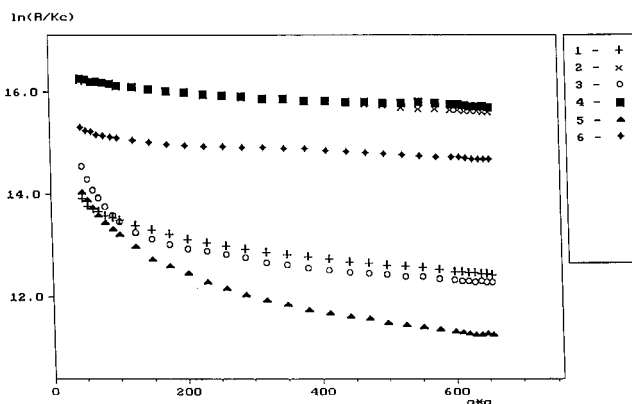


**Figure 3.** Guinier plot of the scattering intensities of AIFL samples in water ( $c = 1$  g/L): 1, AIFL1, 33 °C; 2, AIFL1, 34 °C; 3, AIFL2, 32 °C; 4, AIFL2, 33 °C; 5, AIFL6, 43 °C; 6, AIFL6, 45 °C.

**Table 3. Apparent Values of the Structural Parameters of AIFL1, -2, and -6 below and above the Phase Transition Temperature**

sample	temp (°C)	$10^{-6} M_w$ (g/mol)	$\langle R_G^2 \rangle_z^{1/2}$ (nm)	$\rho$ (g/mL)
AIFL1	33	1.7	181	$1.1 \times 10^{-4}$
	34	12.0	66	$1.7 \times 10^{-2}$
AIFL2	32	7.4	314	$9.5 \times 10^{-5}$
	33	13.6	99	$5.6 \times 10^{-3}$
AIFL6	43	3.2	262	$7.1 \times 10^{-5}$
	45	5.5	133	$9.3 \times 10^{-4}$

phase transition temperature increased, while anionically modified copolymers did not show any phase transition effect, at least in the range of our measurements (<90 °C) and at a pH value of 7.

A comparable behavior was found for complexes from PNIPAM and ionic surfactants.<sup>18–20</sup> Cationic bound surfactants have a much smaller effect on the LCST than anionic ones.

For comparison with the turbidimetric studies SLS investigations were carried out for the samples AIFL1, -2, -4, and -6 in pure water (concentration: 1 g/L), although such measurements of polyelectrolytes do not give correct information about the molecular parameters of the scattering species, because of the long-range Coulomb interactions. While for AIFL4 a significant change in the scattering behavior could not be observed up to 60 °C, the other samples showed a steep increase of the scattering intensity at a critical temperature in very good agreement with the findings of turbidimetry. This increase is connected with a clearly pronounced change of the shape of the scattering function, as demonstrated by a Guinier plot<sup>21</sup> of the Rayleigh ratios  $R(q)$  of the scattering intensities in Figure 3 ( $\ln R(q)/Kc$ ) versus  $q^2$ ;  $K$  = contrast factor,  $c$  = mass concentration of the scattering species,  $q = (4\pi/\lambda) \sin \theta/2$ ,  $\lambda$  = wavelength in the medium,  $\theta$  = scattering angle). The scattering curves were recorded about 0.5 °C below and above the switching temperature. By extrapolation to the zero scattering angle one can determine apparent values of the weight average of particle mass  $M_w$  and the  $z$ -average of the square of the radius of gyration  $\langle R_G^2 \rangle_z$ . The essential changes consist in a slight aggregation and a transition to much more compact structures. The structure density can be roughly estimated using the model of a equivalent sphere with the radius  $\langle R_G^2 \rangle_z^{1/2}$ . The parameters obtained by extrapolating the initial ranges of the scattering functions by a second-order fit are collected in Table 3. For the



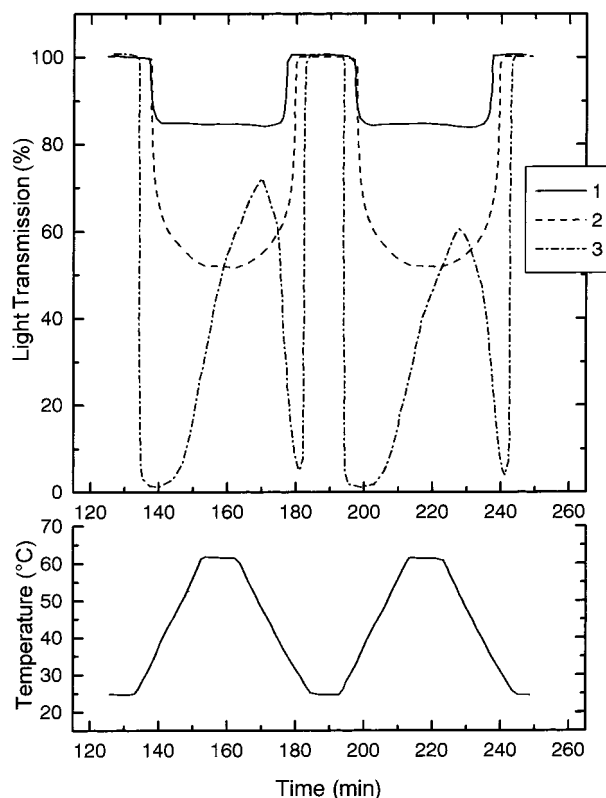


**Figure 4.** Influence of sodium chloride concentration on phase transition behavior of sample AIFL2, polymer concentration 2 g/L: 1, H<sub>2</sub>O; 2, 0.1 M NaCl; 3, 0.5 M NaCl.

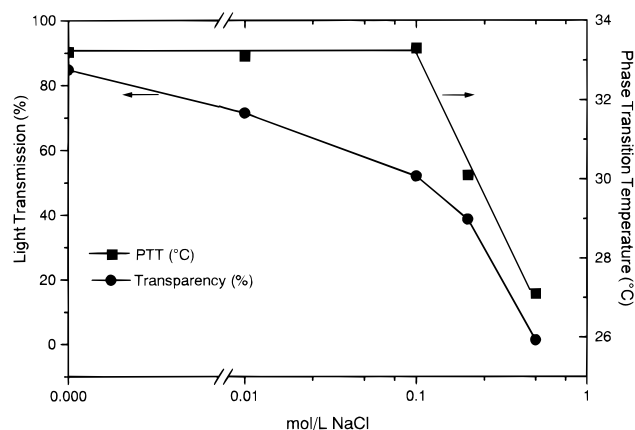


**Figure 5.** Dependence of the phase transition temperature (PTT) and the light transmission at  $T > \text{PTT}$  on the sodium chloride concentration for AIFL2 ( $c = 2$  g/L).

systems below the transition temperature the strong curvature of the scattering curves allows only a rough estimation of the structural parameters. The switch-over between the structures could be reversibly realized by changes in temperature of about 1 °C.

**(ii) Studies in Aqueous Sodium Chloride Solutions.** The behavior of ionically modified LCST polymers in aqueous solutions of a low molecular electrolyte was studied in detail with the copolymer sample AIFL2.

The influence of the addition of a low molecular salt (NaCl) on the phase transition temperature and on the turbidity effect at  $T > \text{LCST}$  is demonstrated in Figures 4 and 5. At low salt contents ( $c_{\text{NaCl}} \leq 0.1$  mol/L) the cloud point temperature remains nearly constant to that in pure water, but it drops when the salt concentration is increased to 0.5 mol/L (27.1 °C). At higher salt

concentration (1 mol/L) this polymer precipitates even at room temperature.

Furthermore, the turbidity at  $T > \text{LCST}$  increases continuously with increasing salt concentration. For 0.5 mol/L NaCl, the initially turbid solution obtained above the cloud point temperature becomes again more transparent (Figure 4) with further heating. This is caused by secondary aggregation of the polymer particles to large visible flakes and the transition to an optically inhomogeneous system. During cooling this flakes disintegrate to the primary particles, which dissolve at the LCST.

The observed strong influence of the salt content on the phase transition behavior and on the primary particles formed above the cloud point temperature can be explained by the assumption that in salt-free or low salt-containing solutions the unscreened ionic charges partly prevent the polyelectrolyte chains from collapsing, whereas at higher electrolyte concentration this polyelectrolyte behavior is increasingly suppressed.

The temperature and ionic strength dependencies of the intrinsic viscosity  $[\eta]$  and the Huggins coefficient  $k_H$  are given in Table 4. In general, as expected for polyelectrolytes, the absolute values of  $[\eta]$  decrease with the ionic strength of the solvent. A remarkable decrease of  $[\eta]$  was observed with increasing temperature. With enhanced ionic strength of the solvent this effect becomes more and more pronounced, as it is demonstrated for the sample AIFL2. For the high ionic strength (0.5 M NaCl) a detailed analysis of the temperature dependence of the viscosity data was carried out. Figure 6 represents the corresponding Huggins plot in a double logarithmic presentation. This plot was chosen in order to demonstrate more significantly the change of the concentration dependence at different temperatures. The Huggins coefficients obtained as usually according to eq 1 show a moderate increase up to the cloud point temperature but strong enhanced  $k_H$ -values occur above this temperature, indicating a dramatic change to bad solution properties. The change of the intrinsic viscosity with temperature offers an additional possibility in determining the phase transition temperature. Figure 7 depicts this dependence for the copolymers AIFL2 and AIFL4. The minimum of  $d[\eta]/dT$  corresponds to the phase transition temperature.

Even in the case of AIFL4, where neither a visible cloud point nor a minimum of  $d[\eta]/dT$  reveals a phase transition, the decrease of the intrinsic viscosity indicates a change in the solution behavior. However, for this copolymer  $k_H$  decreases only slightly with temperature in the whole range.

To judge the temperature behavior of the sample AIFL2 more in detail, the scattering intensity of a set of solutions of the concentrations 0.5, 1, 1.5, 2, and 2.5 g/L were measured at 20, 25, and 27 °C. The results were evaluated by Zimm plots<sup>21</sup> according to the expression

$$Kc/R(q) = 1/M_w + 2A_2c + 1/3\langle R_G^2 \rangle_z M_w^{-1} q^2 \quad (2)$$

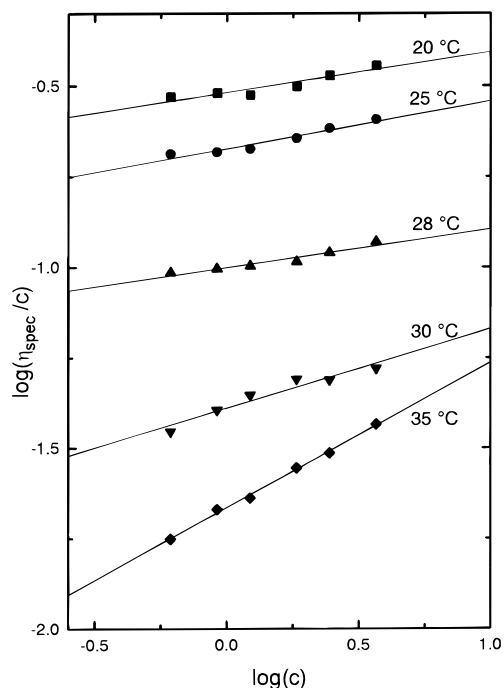
where  $A_2$  is the second virial coefficient.

Figure 8a shows the Zimm diagram measured at 20 °C. The curvature in the small-angle range and the decreasing slope of the concentration dependence with decreasing scattering angle are caused by traces of particulate material, remaining despite the sharp filtration in the solutions. Interpreting the scattering curves

**Table 4.** Influence of Ionic Strength and Temperature on Intrinsic Viscosity  $[\eta]$  (in mL/g) and Huggins Coefficient  $k_H$  of the Cationic Copolymer AIFL2, the Anionic Copolymer AIFL4, and the NIPAM Homopolymer AIFL7

temp (°C)	AIFL2								AIFL4		AIFL7	
	water		0.01 M NaCl		0.1 M NaCl		0.5 M NaCl		0.5 M NaCl		0.5 M NaCl	
	$[\eta]$	$k_H$	$[\eta]$	$k_H$	$[\eta]$	$k_H$	$[\eta]$	$k_H$	$[\eta]$	$k_H$	$[\eta]$	$k_H$
20	(6100) <sup>a</sup>	nd	684	0.38	329	0.45	251	0.46	313	0.40	236	0.57
25							188	0.64				
26											141	0.62
28							92	0.80			c	
30	(5800) <sup>a</sup>	nd					36	3.98	269	0.40	c	
35	(5500) <sup>a</sup>	nd	562	0.44	194	0.57	16	25.10			c	
40							c		189	0.23	c	
50							c		≈50	(0) <sup>b</sup>	c	

<sup>a</sup> Nonlinear Huggins plot due to polyelectrolyte effects. <sup>b</sup> Large scattering of data with nearly zero slope. <sup>c</sup> Not detectable because of strong precipitation.

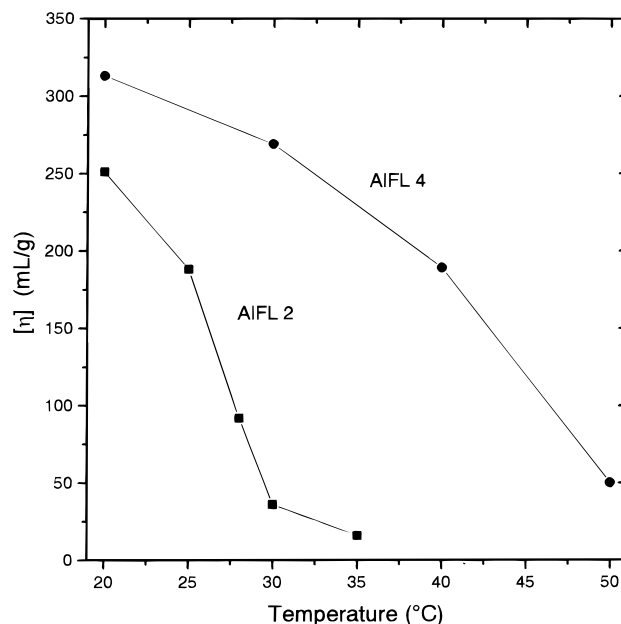
**Figure 6.** Concentration dependence of the reduced viscosity (log-log Huggins plot) of AIFL2 in 0.5 M NaCl at various temperatures.

as bimodal systems, we obtained after a theoretical curve separation<sup>22</sup> the Zimm plot of Figure 8b.

The separation procedure is based on the assumption that the particulate component mainly influences the small-angle range. Starting with an extrapolation of the scattering curves from the wide-angle range, one obtains a first approximation of the contribution of the molecularly dissolved component. If this contribution is subtracted from the measured intensity, the particulate component can be estimated. An iteration leads to a splitting of the scattering curves in the two components.

The parameters extracted from the Zimm diagrams are collected in Table 5. The decrease in  $A_2$  with rising temperature  $T$  indicates the switch-over temperature as lower critical solution temperature. An increase of  $T$  above 27 °C leads to macroscopic flocculation; i.e., the presence of salt causes a decrease of the LCST in comparison to water by 6 °C. Already at 27 °C we found a slightly enhanced  $M_w$ .

To study the structures above the LCST we must dilute the solution up to  $5 \times 10^{-5}$  g/mL, because of the high level of aggregation. The scattering curves mea-

**Figure 7.** Intrinsic viscosity vs temperature for AIFL2 and AIFL4 in 0.5 M NaCl.

sured at 27, 28, and 33 °C are represented in Figure 9 in a scaled double logarithmic plot:  $\log R(q)/(Kc)$  versus  $\log q$ . An improved algorithm basing on a comparison of the experimental scattering curves with theoretically calculated ones for various basic structure types (assuming a logarithmic distribution function for describing the polydispersity) allows one to estimate the structure type and the polydispersity and to determine the structural parameters  $M_w$  and  $R_G$  and for spheres the radius  $a_m$ , which is related to  $M_w$  by  $M_w = (4\pi/3)\rho N_A a_m^3$ , where  $N_A$  is Avogadro's number and  $\rho$  is the average structure density (for details see refs 23 and 24). This fitting procedure uses all measured points for the interpretation of the scattering curves. Data analysis of the curves in Figure 9 shows that the curve at 27 °C may be described by Gaussian coils (except the small-angle range), while the other two curves correspond to the scattering of polydisperse systems of spheres. The structural parameter obtained are given in Table 6. Even at this low polymer concentration the level of aggregation above the LCST is higher than a factor 1000. Obviously, the structures in pure water are protected against higher aggregation by the Coulomb repulsion, while the presence of NaCl screens these interactions, leading to large and very compact particles.

This situation is also reflected by the sedimentation coefficients, which increase continuously between 20

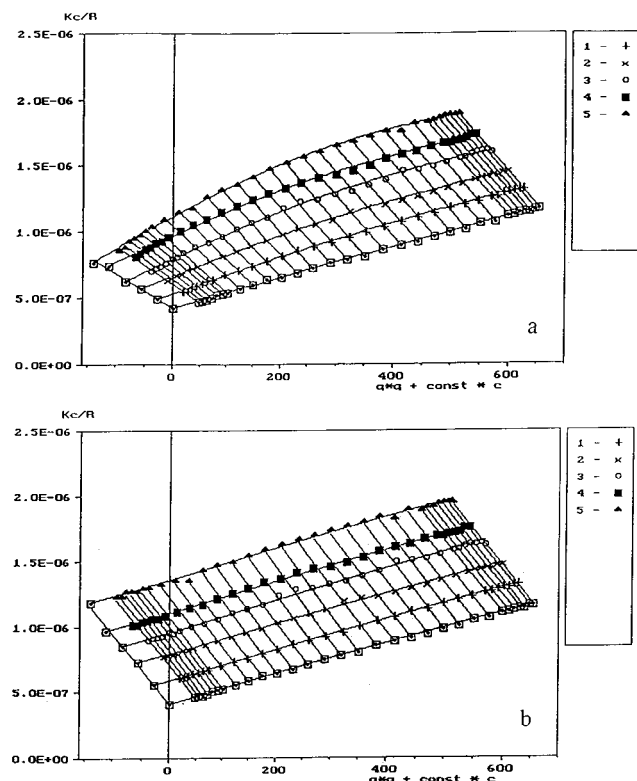


**Figure 8.** Zimm diagram of AIFL2 in 0.5 M NaCl, with  $c =$  (1) 0.5, (2) 1, (3) 1.5, (4) 2, (5) 2.5 g/L: (a) original measured one; (b) after theoretical separation of the contribution of particulate material.

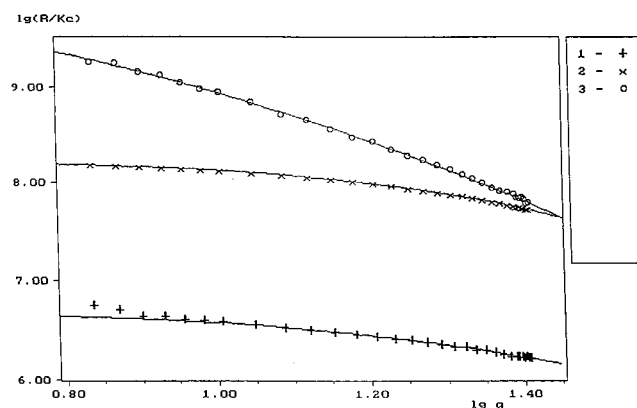


**Figure 9.** Scaled double logarithmic plot of the scattering intensity of AIFL2 ( $c = 5 \times 10^{-2}$  g/L) in 0.5 M NaCl at different temperatures: 1, 27 °C; 2, 28 °C; 3, 33 °C.

**Table 5. Parameters of AIFL2 Obtained from Zimm Diagrams in 0.5 M NaCl at Different Temperatures**

temp (°C)	$10^{-6}M_w$ (g/mol)	$\langle R_G^2 \rangle_z^{1/2}$ (nm)	$10^7 A_2$ ((mol·L)/g <sup>2</sup> )
20	2.4	92	1.5
25	2.5	78	0.64
27	3.0	80	0.23

and 28 °C. At the same time the distribution  $g(s)$  becomes broader due to beginning aggregation of the macromolecules (see Figure 10). At  $T > \text{LCST}$  a bimodal  $g(s)$  distribution occurs, and for  $T > 30$  °C  $s_{\text{app}}$  increases strongly, probably caused by a secondary aggregation process.

The partial specific volume  $\bar{v}$  is nearly independent of the temperature with a slight tendency to increase at  $T > \text{LCST}$ .

**Table 6. Structural Parameters of AIFL2, with  $c = 5 \times 10^{-5}$  g/mL at Different Temperatures (°C)**

temp	struct type	$M_w$ (g/mol)	$\langle R_G^2 \rangle_z^{1/2}$ (nm)	$\sigma^a$	$a_m, s_m^b$ (nm)	$\rho$ (g/mL)
27	coils	$4.8 \times 10^6$	94	0.6	78	0.004
28	spheres	$1.7 \times 10^8$	91	0.45	71	0.19
33	spheres	$1.1 \times 10^{10}$	700	0.7	265	0.23

<sup>a</sup> Polydispersity parameter of a logarithmic distribution function, for coils regarding  $M$ , for spheres regarding radius  $a$ . <sup>b</sup>  $a_m$  = radius of a sphere, corrected for polydispersity;  $s_m$  = radius of gyration of a coil, corrected for polydispersity.

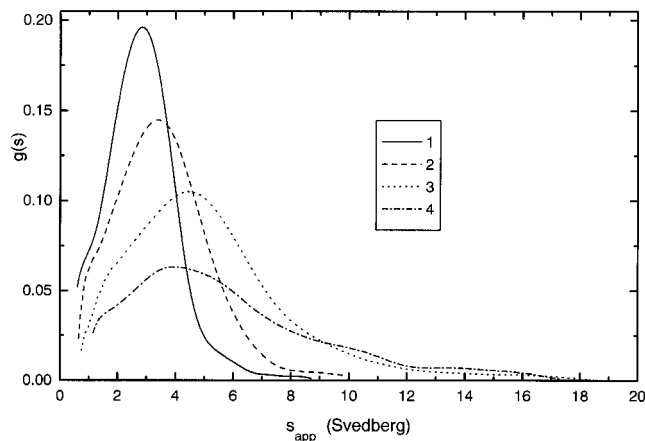


**Figure 10.** Distribution of sedimentation coefficients of AIFL2 (1.8 g/L in 0.5 M NaCl) at various temperatures: 1, 20 °C; 2, 24 °C; 3, 28 °C; 4, 30 °C.

The sedimentation equilibrium experiment at 20 °C was used for an independent absolute determination of the molecular mass of the sample AIFL2. The weight and  $z$ -averaged molecular masses  $M_w$  and  $M_z$  and the second virial coefficient  $A_2$  were estimated from the equilibrium concentration profiles at different cell filling concentrations  $c_0$  according to

$$M_{w,\text{app}} = \frac{1}{\lambda} \frac{c_b - c_m}{c_0} \quad (3)$$

$$M_{z,\text{app}} = \frac{1}{\lambda} \frac{c_b (d(\ln c)/dx)_b - c_m (d(\ln c)/dx)_m}{c_b - c_m} \quad (4)$$

( $\lambda = (1 - \bar{v}\rho_0)\omega^2(r_b^2 - r_m^2)/2RT$  with  $\bar{v}$  = partial specific volume of the solute,  $\rho_0$  = density of the solvent,  $\omega$  = rotor speed in rad/s,  $r_b$  and  $r_m$  are radial positions of cell bottom and meniscus, respectively, and  $x = (r^2 - r_m^2)/(r_b^2 - r_m^2)$  is a dimensionless radial parameter), and

$$\frac{1}{M_{w,\text{app}}} = \frac{1}{M_w} + 2A_2c_0 \quad (5)$$

The calculated values of  $M_w$  and  $A_2$  (see Table 7) are in good agreement with the results from light scattering experiments. The  $M_z/M_w$  value of about 1.3 represents the normal polydispersity of a Flory–Schulz distribution.

When the rotor temperature was increased during the equilibrium experiment, a complete reorientation of the distribution of the polymer concentration within the cells took place. After equilibration (>24 h) the new concentration profile was scanned and then the temperature was increased to the next measuring point. The results of sedimentation equilibrium analysis for 20, 25, 28, and 30 °C are given in Table 7.

**Table 7. Results of Sedimentation Analysis for Sample AIFL2 in 0.5 M NaCl at Various Temperatures ( $s_{app}$  from Sedimentation Velocity,  $M_w$ ,  $M_z$  and  $A_2$  from Sedimentation Equilibrium;  $c_A$  = Estimated Amount of Aggregates) and the Partial Specific Volumes  $\bar{v}$  in H<sub>2</sub>O and 0.5 M NaCl**

$T$ (°C)	$s_{app}$ (Svedberg)	$10^{-6}M_w$ (g/mol)	$10^{-6}M_z$ (g/mol)	$10^7 A_2$ (mol·L/g <sup>2</sup> )	$c_A$ (%)	$\bar{v}$ in H <sub>2</sub> O (mL/g)	$\bar{v}$ in 0.5 M NaCl (mL/g)
20	2.85	2.1	2.7	1.50	0	0.835	0.870
24	3.4						
25		1.5	2.8	0.53	29	0.827	0.859
28	4.7	0.9	2.3	-0.45	57		
30	3.9/13.7	0.4	2.7	-0.35	81	0.828	0.878
32	810						
35						0.839	0.902
40						0.844	

Since the rotor speed was kept constant during the whole equilibrium run, it must be assumed that heavy aggregates, which were formed with increasing temperature, sediment to the cell bottom and do not further contribute to the equilibrium concentration profiles. Thus, the evaluated data for  $M_w$ ,  $M_z$ , and  $A_2$  correspond only to the molecularly dispersed part of the polymer. With increasing aggregation, the use of the initial cell loading concentration  $c_0$  instead of the effective concentration results in too low  $M_w$  values, because the calculation of  $M_w$  is directly related to  $c_0$  (eq 3).

Therefore, the decrease of  $M_w$  in Table 7 compared with the value at 20 °C can be used for a rough estimation of the mass fraction of aggregates  $c_A = 1 - M_w(T)/M_w(20\text{ °C})$  in the solutions of higher temperatures.

On the other hand, the calculation of  $M_z$ , which depends on concentration only in terms of the differences between cell bottom and meniscus concentration  $c_b$  and  $c_m$  and the corresponding slopes of the radial concentration distribution (see eq 4), is less sensitive to errors in the cell loading concentration. The same is true for the determination of the second virial coefficient  $A_2$  from the concentration dependence of  $M_{w,app}$  (eq 5).

With increasing temperature the second virial coefficient from sedimentation equilibrium experiments decreases in the same manner as the  $A_2$  from light scattering and reaches negative values for  $T > \text{LCST}$ . This is in accordance with the high  $k_H$  values from viscometry.

### (iii) Studies in Water/Organic Solvent Mixtures.

Comparative investigations were performed about the behavior of the ionically modified NIPAM copolymers in mixed solvents, varying solvent composition and temperature. We studied both kinds of samples, characterized by the existence or absence of a LCST as it is described for the copolymers AIFL2 and AIFL3. Dimethylformamide (DMF) is an appropriate organic solvent for these studies, because both copolymers are soluble in it. In Figure 11a,b the results of viscosimetric measurements in 0.1% solutions of the copolymers are shown in dependence on temperature at various water/DMF ratios. Only small differences occurred in the specific viscosity values with a slight decrease with increasing temperature for the anionic derivative. In comparison with it, a dramatic changed behavior was found in the case of the cationic modified copolymer sample. Markedly different absolute viscosity values and the existence of viscosity maxima at an excess of water in the solvent mixture, accompanied by the appearance of phase separation (the solutions became turbid), characterize the course of the viscosity-tem-

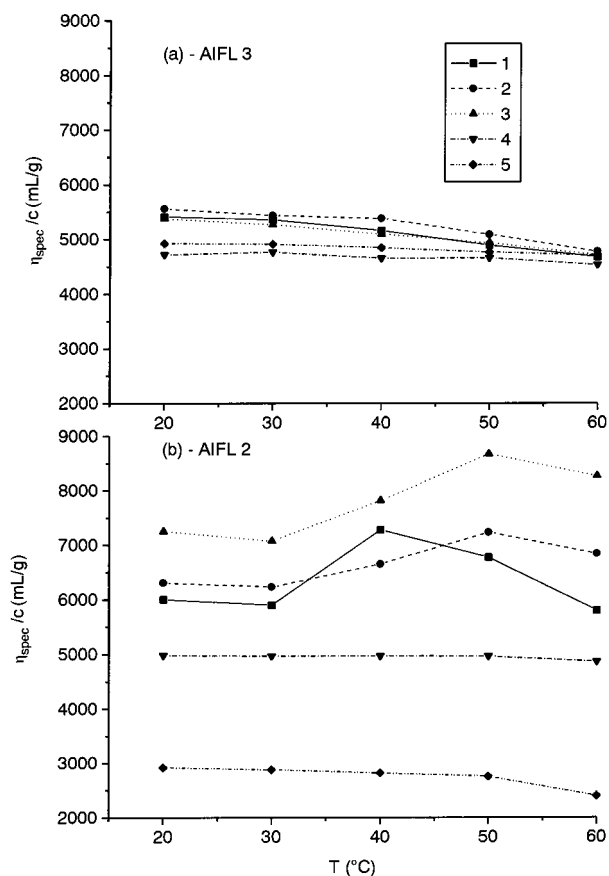


**Figure 11.** Dependence of the reduced viscosities of NIPAM-copolymer solutions (1 g/L) on temperature in various water/DMF mixtures of (1) water, (2) 9:1, (3) 7.5:2.5, (4) 5:5, (5) 0.5:9.5 weight fractions of water/DMF: (a) AIFL3; (b) AIFL2.

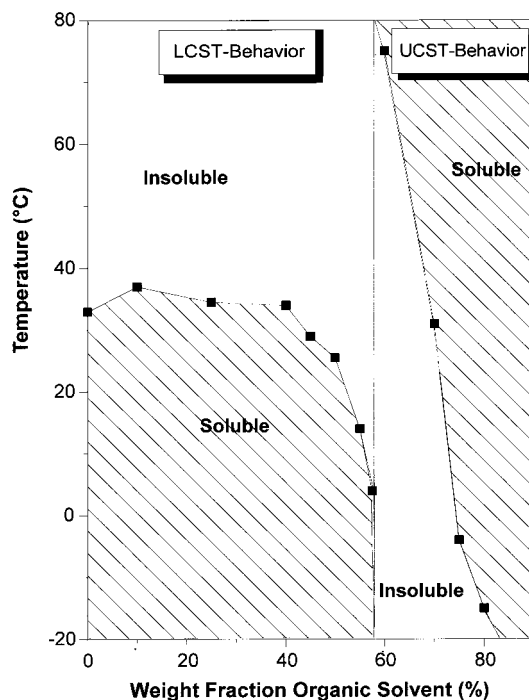


**Figure 12.** Phase diagram of AIFL2 ( $c = 5$  g/L) in water/DMF mixtures.

perature curves of this NIPAM copolymer. Figure 12 presents the dependence of the cloud point temperature on solvent composition. Up to 40% of DMF the LCST remains nearly constant, and then a steady decrease



to a level near 0 °C at 58% DMF takes place. With higher fractions of DMF in the solvent mixture the cationic NIPAM copolymer shows opposite solution properties; the normal UCST behavior (upper critical solution temperature) was found. At 60% DMF the copolymer is insoluble below 70 °C. With rising amount of DMF the UCST decreases strongly up to values below 0 °C.

## Conclusion

Ionically modified NIPAM copolymers were synthesized by free radical polymerization. Due to the comparable reactivity ratios of the various used acrylic derivatives, sufficiently narrow molecular weight and composition distributions could be obtained. The fraction of ionic units in the copolymers was adjusted to about 6–7 mol %.

In aqueous solutions, cationically modified products but also a sample containing an ampholytic betaine structure showed phase separation upon heating, whereas for the anionically charged products this behavior could not be observed. The different properties can be explained by a markedly higher hydrophobicity of the cationic groups. This is indicated by the fact that the copolymerization of acrylamide with cationically modified acrylamide derivatives, used in our investigations, runs as a precipitation polymerization at sufficiently high salt content in aqueous solution.<sup>25</sup> A corresponding sensitivity against added salt was also observed in the phase transition behavior.

Phase transition was found to be initiated by conformational changes of the dissolved macromolecules still below the cloud point temperature followed by aggregation and phase separation. Phase-separated ionic copolymers form colloidal particles which are electrostatically stabilized in pure water. At higher salt concentrations in the solvent the particles become increasingly less stable due to the enhanced suppression of the Coulomb interactions.

Phase transition behavior took also place in mixtures of water and dimethyl formamide. Above 60 wt % DMF

the cationically modified copolymer AIFL2 showed UCST properties.

## References and Notes

- (1) Taylor, L. D.; Ceranowski, L. D. *J. Polym. Sci.* **1975**, *23*, 259.
- (2) Russo, P. S., Ed. *Reversible Polymer Gels & Related Systems*; ACS Symposium Series 350; American Chemical Society: Washington, DC, 1987.
- (3) Bae, Y.; Okano, T.; Kim, S. W. *J. Polym. Sci., Polym. Phys. Ed.* **1990**, *28*, 923.
- (4) Ringsdorf, H.; Simon, J.; Winnik, F. M. *Macromolecules* **1992**, *25*, 5353.
- (5) Chen, G.; Hoffman, A. S. *Nature* **1995**, *373*, 49.
- (6) Heskins, M.; Guillet, J. E. *J. Macromol. Sci. Chem.* **1986**, *A-2*, 1441.
- (7) Guillet, J. E.; Heskins, M.; Murray, D. G. U.S. Pat. 4,536,294, 1985.
- (8) Shalaby, S. W. In *Water Soluble Polymers*; (Eds. Shalaby, S. W., McCormick, C. L., Butler, G. B., Eds.; ACS Symposium Series 467; Washington, DC, 1991; p 502.
- (9) Inomata, H.; Goto, S.; Otake, K.; Saito, S. *Langmuir* **1992**, *8*, 687.
- (10) Schild, H. G.; Tirrell, D. A. *J. Phys. Chem.* **1990**, *34*, 4352.
- (11) Arai, K.; Kawabata, Y. *Makromol. Chem., Rapid Commun.* **1995**, *16*, 875.
- (12) Dong, L. C.; Hoffman, A. S. *J. Controlled Release* **1991**, *15*, 141.
- (13) Deng, Y. L.; Pelton, R. *Macromolecules* **1995**, *28*, 4617.
- (14) Hu, Y.; Armentrout, R. S.; McCormick, C. L. *Polym. Prepr.* **1996**, 661.
- (15) Lundstedt, L. G.; Ile, G.; Schulz, W. F. U.S. Pat. 2,697,113 (Wyandotte Chemicals Corp.), Dec 14, 1954.
- (16) Stafford, W. F. *Anal. Biochem.* **1992**, *203*, 295.
- (17) Gornitz, E.; Hahn, M.; Jaeger, W.; Dautzenberg, H. *Prog. Colloid Polym. Sci.* **1997**, *107*, 127.
- (18) Schild, H. G.; Tirrell, D. A. *Polym. Prepr. (Am. Chem. Soc., Div. Polym. Chem.)* **1989**, *30* (2), 350.
- (19) Tam, K. C.; Ragaram, S.; Pelton, R. H. *Langmuir*, **1994**, *10*, 418.
- (20) Kokufuta, E.; Zhang, Y.; Tanaka, T.; Mamada, A. *Macromolecules* **1993**, *26*, 1053.
- (21) Kerker, M. *The Scattering of Light and other Electromagnetic Radiation*; Academic Press: New York, 1969.
- (22) Dautzenberg, H.; Rother, G. *J. Appl. Polymer Sci., Appl. Polym. Symp.* **1991**, *48*, 351.
- (23) Dautzenberg, H.; Rother, G. *J. Polym. Sci., Polym. Phys. Ed., Part B* **1988**, *76*, 353.
- (24) Dautzenberg, H.; Rother, G. *Makromol. Chem., Macromol. Symp.* **1992**, *61*, 94.
- (25) Ramesh, M.; Cramm, J. R. EP 0 637 598 A3 (NALCO Chem. Co.), June 10, 1995.

MA9800010